

## Discovery of A-1331852, a First-in-Class, Potent, and Orally-Bioavailable BCL-X<sub>L</sub> Inhibitor

Le Wang, George A. Doherty, Andrew S. Judd,\* Zhi-Fu Tao, T. Matthew Hansen, Robin R. Frey, Xiaohong Song, Milan Bruncko, Aaron R. Kunzer, Xilu Wang, Michael D. Wendt, John A. Flygare, Nathaniel D. Catron, Russell A. Judge, Chang H. Park, Shashank Shekhar, Darren C. Phillips, Paul Nimmer, Morey L. Smith, Stephen K. Tahir, Yu Xiao, John Xue, Haichao Zhang, Phuong N. Le, Michael J. Mitten, Erwin R. Boghaert, Wenqing Gao, Peter Kovar, Edna F. Choo, Dolores Diaz, Wayne J. Fairbrother, Steven W. Elmore, Deepak Sampath, Joel D. Levenson, and Andrew James Souers



Cite This: *ACS Med. Chem. Lett.* 2020, 11, 1829–1836



Read Online

ACCESS |



Metrics & More



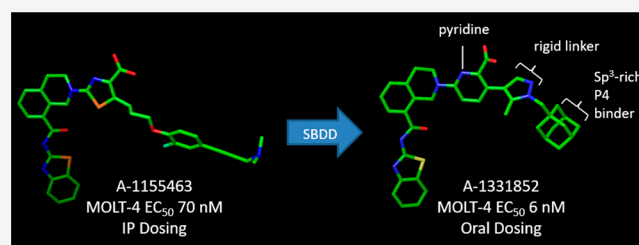
Article Recommendations



Supporting Information

**ABSTRACT:** Herein we describe the discovery of A-1331852, a first-in-class orally active BCL-X<sub>L</sub> inhibitor that selectively and potently induces apoptosis in BCL-X<sub>L</sub>-dependent tumor cells. This molecule was generated by re-engineering our previously reported BCL-X<sub>L</sub> inhibitor A-1155463 using structure-based drug design. Key design elements included rigidification of the A-1155463 pharmacophore and introduction of sp<sup>3</sup>-rich moieties capable of generating highly productive interactions within the key P4 pocket of BCL-X<sub>L</sub>. A-1331852 has since been used as a critical tool molecule for further exploring BCL-2 family protein biology, while also representing an attractive entry into a drug discovery program.

**KEYWORDS:** BCL-X<sub>L</sub>, BCL-2, apoptosis, A-1331852, A-1155463, structure-based drug design (SBDD)



Despite the inherent challenges in generating effective small molecule antagonists of the antiapoptotic BCL-2 family proteins, significant progress has been made in recent years. ABT-737 and the related orally bioavailable compound ABT-263 (navitoclax) were reported as the first BH3 mimetics that bind with high affinity to BCL-2, BCL-X<sub>L</sub>.<sup>1,2</sup> In preclinical models of both solid and hematological cancers, navitoclax inhibits tumor growth as a single agent<sup>3</sup> and in combination with multiple chemotherapeutic and targeted agents.<sup>4,5</sup> In clinical studies, navitoclax exhibited objective antitumor activity in lymphoid malignancies believed to be dependent upon BCL-2 for survival, yet it also induced rapid, reversible, and concentration-dependent thrombocytopenia<sup>6,7</sup> that was determined to be a consequence of BCL-X<sub>L</sub> inhibition.<sup>8,9</sup> The latter experience and discovery prompted not only alterations in clinical dosing of navitoclax but also the development of ABT-199/GDC-0199 (venetoclax), a BCL-2-selective inhibitor that maintains efficacy in hematologic tumor models while sparing platelets.<sup>10</sup> Venetoclax first demonstrated objective responses in chronic lymphocytic leukemia (CLL)<sup>11</sup> without dose limiting thrombocytopenia, thus providing validation for selective BCL-2 inhibition in the clinic.

Navitoclax has also been evaluated clinically for the treatment of solid tumors believed to be predominantly dependent on BCL-X<sub>L</sub> for survival.<sup>5,12</sup> When combined with

docetaxel and other chemotherapeutic regimens, neutropenia and febrile neutropenia above and beyond what was expected from chemotherapy alone were observed in multiple patients,<sup>12</sup> thus limiting the navitoclax exposure and efficacy that could be observed in specific settings. We hypothesized that the BCL-2 inhibitory activity of navitoclax was exacerbating the neutropenic toxicity of these chemotherapies.<sup>13</sup> This prompted the further hypothesis that a BCL-X<sub>L</sub> selective inhibitor could maintain efficacy in BCL-X<sub>L</sub> dependent solid tumors when combined with chemotherapy while avoiding the dose-limiting neutropenia observed with combinations such as navitoclax plus docetaxel in the clinic. Furthermore, as the clinical development of navitoclax continued with other types of agents across different disease states, we envisioned that a BCL-X<sub>L</sub> selective inhibitor could provide a complementary option for targeting this key protein.

In order to test these hypotheses we first generated A-1155463 (1, Figures 1 and 2), a BCL-X<sub>L</sub> inhibitor that shows

**Special Issue:** Medicinal Chemistry: From Targets to Therapies

**Received:** December 2, 2019

**Accepted:** March 30, 2020

**Published:** March 30, 2020



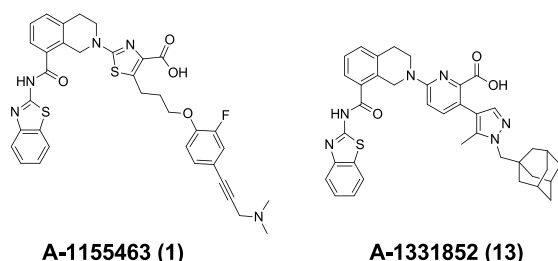


**Figure 1.** Chemical structures of BCL- $X_L$  inhibitors A-1155463 (1) and A-1331852 (13).

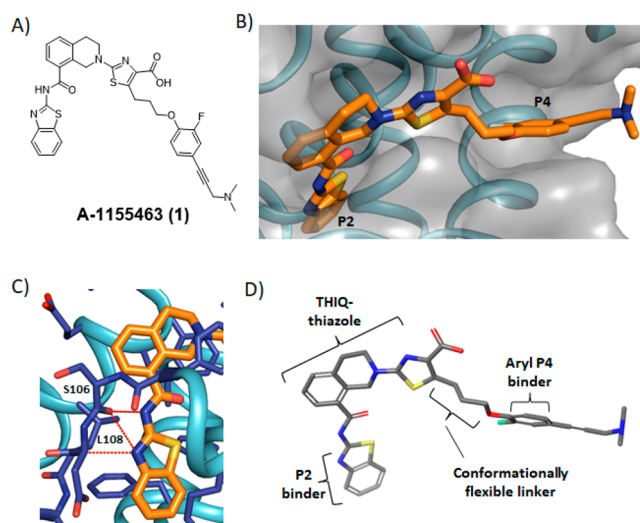


**Figure 2.** (A) Chemical structure of BCL- $X_L$  inhibitor A-1155463 (1). (B) X-ray crystal structure of A-1155463 bound to BCL- $X_L$  protein, highlighting key P4 and P2 binding pockets. BCL- $X_L$  protein is depicted as a ribbon with a gray surface. (C) Depiction of the benzothiazole moiety of A-1155463 bound to Ser106 and Leu108 in the BCL- $X_L$  P2 pocket. BCL- $X_L$  protein is depicted as a ribbon with key amino acid residues labeled. (D) Rendering of A-1155463 bioactive conformation bound to BCL- $X_L$  protein.

robust potency against BCL- $X_L$ -dependent human tumor lines while sparing BCL-2- and MCL-1-dependent cell lines.<sup>14</sup> The on-target potency and selectivity of this molecule allowed for several investigations into BCL- $X_L$  biology.<sup>13,15,16</sup> For example, in NSCLC cell lines, the combination of docetaxel with A-1155463, but not the BCL-2 selective inhibitor venetoclax (ABT-199), replicated the cell killing synergy of docetaxel plus navitoclax; these data supported the hypothesis that BCL- $X_L$  inhibition alone could combine with chemotherapy to kill solid tumor cells. Administration of this molecule to mice demonstrated rapid thrombocytopenia and modest tumor growth inhibition in a xenograft model of SCLC (H146), thus providing the first characterization of a selective BCL- $X_L$  inhibitor *in vivo*.<sup>14</sup> Ultimately, the poor solubility and oral absorption of this molecule limited its utility for more advanced *in vivo* experiments.

We were thus interested in generating a selective BCL- $X_L$  inhibitor that could be deployed as an oral agent in additional *in vivo* efficacy and exploratory toxicology studies, while additionally serving as the basis for a drug discovery program. To this end, we optimized the A-1155463 pharmacophore to afford A-1331852 (13, Figure 1), a highly potent and selective BCL- $X_L$  inhibitor that demonstrates oral activity *in vivo* in

xenograft models of human tumors.<sup>13</sup> Additionally, A-1331852 was used in the key investigative toxicology study demonstrating that neutropenia caused by navitoclax was primarily driven by BCL-2 and not BCL- $X_L$  inhibition.<sup>13</sup> These and other data provided preclinical validation of the hypotheses supporting further development of selective BCL- $X_L$  inhibitors for the treatment of solid tumors. Herein we report the small molecule optimization approach that afforded this compound.

At the onset of this work, our primary goal was to generate molecules with suitable oral absorption that at least maintained the potency and selectivity of A-1155463. While this and other analogs based on the tetrahydroisoquinoline-thiazole core (THIQ-thiazole, 2 in Table 1) showed good *in*

**Table 1.** Tetrahydroisoquinoline Cores 2 (THIQ-thiazole) and 3 (THIQ-pyridine) and Selected Parameters

| Compound | BCL- $X_L$ FRET $K_i$ (nM) | Solution Stability (pH 7.4, 37 °C) |                      |
|----------|----------------------------|------------------------------------|----------------------|
|          |                            | $t_{1/2}$ (days)                   | eLogD <sub>7,4</sub> |
| 2        | 65                         | 58                                 | 3.02                 |
| 3        | 164                        | 63                                 | 2.85                 |

*vitro* profiles, the oral pharmacokinetic properties of compounds in this class were consistently poor.<sup>17</sup> Previous efforts en route to A-1155463 had delineated the requirement for the benzothiazole amide portion of the BCL- $X_L$ -targeting pharmacophore. This moiety makes critical electrostatic interactions with backbone residues Ser106 and Leu108 in helix 3 of the protein that serve to anchor the more hydrophobic interactions in the P2 pocket (see Figure 2C).<sup>14,17,18</sup> Additional modifications directly to the tetrahydro-isoquinoline (THIQ) core also indicated a lack of tolerability for potent BCL- $X_L$  binding.

As we revisited the series with the goal of achieving suitable oral exposure, we reexamined the picolinic acid containing core 3 (THIQ-pyridine, Table 1). This compound exhibited lower target affinity relative to the corresponding THIQ-thiazole 2 yet showed superior pharmacokinetics in rat.<sup>17</sup> Both cores showed good solution stability at pH 7.4, suggesting that amide hydrolysis would not be a significant barrier to achieving oral exposure. Finally, THIQ-pyridine 3 had a slightly lower measured logD, which was a benefit given the anticipation of added lipophilic molecular weight. Using these criteria, we selected 3 as the basis for preliminary SAR generation.

Further examination of the A-1155463 pharmacophore and its BCL- $X_L$ -bound structure<sup>14</sup> prompted a reassessment of the conformationally flexible propoxy unit linking the thiazole to the phenyl P4-binding moiety. As shown in Figures 2B and 2D, the propoxy linker adopts a destabilizing gauche arrangement of atoms in its bound conformation. While we considered tactics to reinforce this acyclic conformation, cyclization of the linker unit offered an intriguing means of biasing an active conformation for the P4 binding unit while

decreasing the number of rotatable bonds. The latter modification, in turn, could impart better drug-like properties such as oral absorption.<sup>19</sup> Finally, the incorporation of heterocyclic linkers specifically could allow for additional opportunities to fine-tune the physicochemical properties of the molecules.

We further reasoned that 5-membered ring heterocycles would afford the optimal vectors into the critical P4 pocket. To this end, we first prepared a set of analogs (**5**, **6**, and **7**) that maintained an unsubstituted phenyl P4-binding moiety attached to specific 5-membered ring heterocycles with increasing nitrogen content to assess the tolerance for polarity in the linker region. The pyrrole-linked compound **5** showed nearly 30-fold improvement in BCL-X<sub>L</sub> affinity relative to the linear compound **4**,<sup>17</sup> while also maintaining selectivity over BCL-2 (Table 2). The pyrazole **6** maintained the favorable

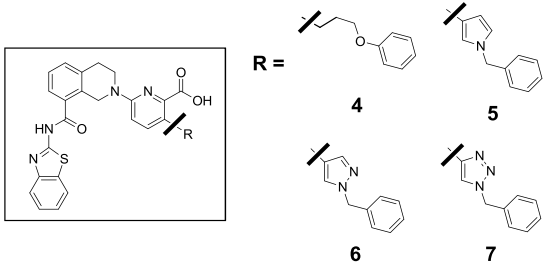
Therefore, the pyrazole **6** was selected for further optimization efforts.

Generation of an X-ray cocrystal structure of a closely related analog of **6** (compound **8**, Figure 3A) with BCL-X<sub>L</sub> provided several structural insights for subsequent rounds of optimization. As shown in Figure 3A, the THIQ-pyridine binds the hydrophobic P2 pocket as described previously, with the new pyrazole linker at a 41° dihedral angle to the picolinate. This in turn provided an efficient vector to the P4 pocket. Analysis of the crystal structure suggested that substitutions to the 3- and 5-positions of the pyrazole could achieve additional hydrophobic interactions with the helix 3 and 2 regions, respectively, of the protein. We additionally postulated that substitutions to these positions could reinforce the ground state population of the pyrazole:pyridine torsion observed in the binding pose.

An additional and surprising observation was the orientation of the terminal pyridine ring of **8** bound within the P4 pocket. This orientation was orthogonal relative to the dimethylamino-propynyl-2-fluorophenyl portion of A-1155463 and other phenyl P4 binders described previously<sup>15</sup> in a related series. As shown in Figures 3A and 3B, the Tyr195 residue of BCL-X<sub>L</sub> bound to **8** rotated to expand the P4 pocket relative to when bound to A-1155463. The Tyr195 residue in the BCL-X<sub>L</sub>:**8** structure thereby adopted a conformation similar to that observed when complexed with ABT-737.<sup>20</sup> However, while the P4-binding region of ABT-737 or navitoclax takes advantage of an intermolecular face-face  $\pi$ -stacking interaction with Tyr195, the pyridine of **8** is situated perpendicular to the Tyr195  $\pi$ -system. These observations indicated that, unlike the linear chain analogs, such as A-1155463, or the acylsulfonamide pharmacophore of navitoclax, pyrazole linker-analogs like **8** may allow for potency gains to be made via P4 interactions without utilization of aromatic moieties and  $\pi$  stacking. Specifically, this crystal structure analysis yielded the possibility of introducing sp<sup>3</sup>-rich cycloalkyl groups that could occupy the lipophilic volume of the P4 pocket. This would represent a significant departure from previously reported tactics and a further opportunity to direct the pharmacophore into more drug-like space.<sup>21,22</sup>

These structural insights thus prompted two specific explorations; the first was to investigate 3- and 5-position substitution on the pyrazole ring, while the second involved the incorporation of nonaromatic P4 binders. To assess the former, we first probed the potential binding interactions that could be made from the 3- and 5-positions of the pyrazole moiety via the generation and biological evaluation of the 3-

**Table 2.** BCL-X<sub>L</sub> and BCL-2 TR-FRET Binding Data of THIQ-Pyridine Analogs 4–7



| Compound | BCL-X <sub>L</sub> FRET K <sub>i</sub> (nM) | BCL-2 FRET K <sub>i</sub> (nM) |
|----------|---|--------------------------------|
| <b>4</b> | 11  | 626                            |
| <b>5</b> | 0.329                                       | 119                            |
| <b>6</b> | 0.296                                       | 117                            |
| <b>7</b> | 5.96  | 348                            |

binding characteristics of pyrrole **5**. In contrast, the triazole analog **7** showed diminished BCL-X<sub>L</sub> binding, suggesting that the polarity of the added nitrogen was not making productive interactions with the protein. Similar SAR efforts with cyclic linkers of different size and content did not yield compounds with improved properties relative to **5** and **6** (data not shown).

Though both **5** and **6** initially displayed potential for further optimization of target affinity, the former compound lost activity upon retest over time, thus indicating instability on storage. This was perhaps not surprising given the known susceptibility of pyrrole moieties to oxidative degradation.

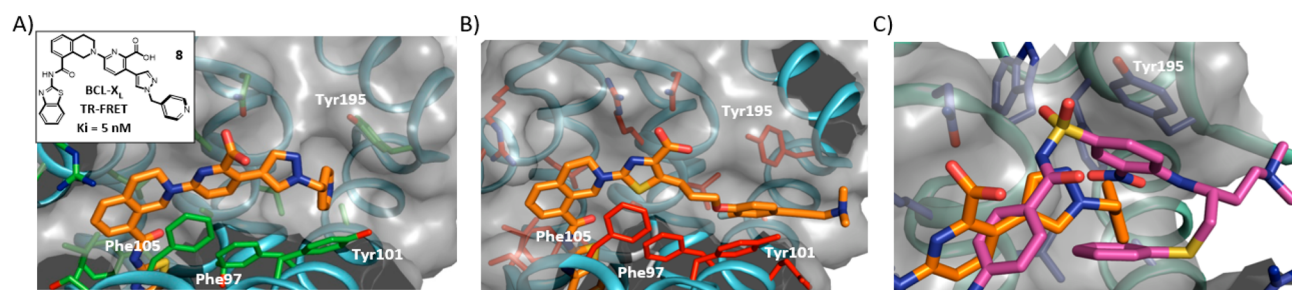
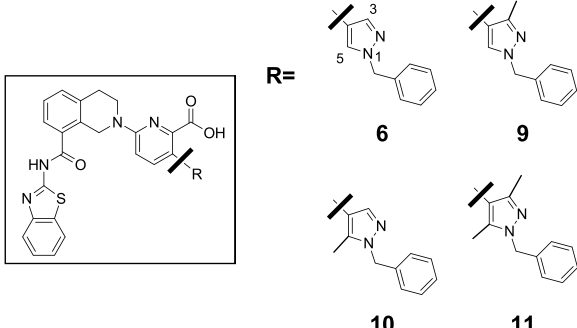


**Figure 3.** (A) X-ray crystal structure of compound **8** bound to BCL-X<sub>L</sub> protein. BCL-X<sub>L</sub> protein is depicted as a ribbon with key amino acid residues colored green; inset depicts the structure of **8**. (B) X-ray crystal structure of compound A-1155463 (**1**) bound to BCL-X<sub>L</sub> protein. Key amino acid residues are colored red.<sup>20</sup> (C) Superposition of **8** and ABT-737 bound to BCL-X<sub>L</sub> protein.



methyl-, 5-methyl-, and 3,5-dimethyl-pyrazoles 9–11. Compound 9 showed similar if not slightly lower target affinity relative to 6 (Table 3). Methylation at the 5-position, however, was clearly beneficial, as analogs 10 and 11 showed an approximately 7- and 11-fold improvement in target affinity relative to parent 6.

**Table 3. BCL-X<sub>L</sub> and BCL-2 TR-FRET Binding Data and *In Vitro* Cell Efficacy of 6 and 9–11**



| Compound | BCL-X <sub>L</sub> FRET K <sub>i</sub> (nM) | BCL-2 FRET K <sub>i</sub> (nM) | MOLT-4 EC <sub>50</sub> (nM, 10% HS) |
|----------|---|--------------------------------|--------------------------------------|
| 6        | 0.30  | 117                            | >5,000                               |
| 9        | 0.65  | 413                            | >5,000                               |
| 10       | 0.027                                       | 70                             | 1,610                                |
| 11       | 0.044                                       | 548                            | >5,000                               |

Since the achieved BCL-X<sub>L</sub>-binding affinity was consistent with potential cellular activity in human cancer cell lines, analogs 9–11 were tested in the BCL-X<sub>L</sub> dependent cell line MOLT-4, as well as the BCL-2 dependent cell line RS4;11. We were encouraged to find that 5-methylpyrazole analog 10 demonstrated low micromolar activity in the MOLT-4 cells in the presence of 10% human serum. All other analogs tested were not effective up to the concentrations assayed.

The modest but encouraging activity of 10 in human tumor cells prompted the evaluation of pharmacokinetic properties in rats. As shown in Table 4, the intravenous (IV) PK of 10 is

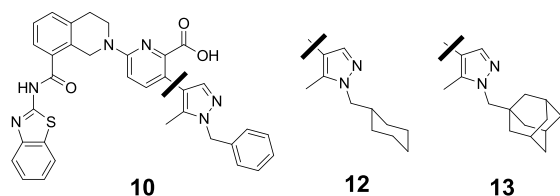
**Table 4. Select Rat PK Parameters for 10**

| Rat IV PK, 5 mpk     |                        |                          |            | Rat PO PK, 5 mpk      |            |       |
|----------------------|------------------------|--------------------------|------------|-----------------------|------------|-------|
| t <sub>1/2</sub> (h) | V <sub>ss</sub> (L/kg) | Cl <sub>p</sub> (L/h/kg) | AUC (μM·h) | C <sub>max</sub> (μM) | AUC (μM·h) | F (%) |
| 9.4                  | 0.29                   | 0.13                     | 71.2       | 5.54                  | 11.7       | 17    |

characterized by low volume of distribution, low total plasma clearance, and a long IV terminal half-life of 9.4 h. Encouragingly, a suitable level of oral absorption was observed, with compound 10 exhibiting 17% oral bioavailability and approximately 3-fold C<sub>max</sub>-coverage (total drug exposure) of the cellular EC<sub>50</sub> after a single low dose of 5 mg/kg.

With an encouraging lead molecule in hand, the incorporation of nonaromatic P4-binding moieties became the next focus. We were particularly attracted to this approach as it would increase the pharmacophore sp<sup>3</sup>-fraction, an attribute that could improve the overall properties of the molecule.<sup>21,22</sup> To test this hypothesis, we first prepared analogs containing either cyclohexane (12) or adamantane (13) P4-binding moieties (Table 5), the latter of which was

**Table 5. BCL-X<sub>L</sub> and BCL-2 TR-FRET Binding Data and *In Vitro* Cell Efficacy of 1, 10, 12, and 13**



|    | BCL-X <sub>L</sub> FRET K <sub>i</sub> (nM) | BCL-2 FRET K <sub>i</sub> (nM) | MOLT-4 EC <sub>50</sub> (nM, 10% HS) | RS4;11 EC <sub>50</sub> (nM, 10% HS) |
|----|---|--------------------------------|--------------------------------------|--------------------------------------|
| 1  | <0.01                                       | 74.0                           | 130                                  | >5,000                               |
| 10 | 0.027                                       | 69.8                           | 1,610                                | >5,000                               |
| 12 | 0.008                                       | 28.5                           | 197                                  | >5,000                               |
| 13 | <0.01                                       | 6.1                            | 6.3                                  | >5,000                               |

intended to maximize the possible sp<sup>3</sup>-driven van der Waals interactions in this pocket. Subsequent biological evaluation indicated that the cyclohexane of 12 was clearly beneficial to the BCL-X<sub>L</sub> binding affinity relative to the benzyl parent 10. This translated into an 8-fold improvement in functional efficacy in the MOLT-4 cell viability assay, with 12 demonstrating an EC<sub>50</sub> of 197 nM. As shown in Table 5, expansion of the P4 cyclohexane to the more sterically demanding adamantane (13) had a remarkable effect on the *in vitro* activity. The cell-killing efficacy of A-1331852 (13) against MOLT-4 cells was improved by 10- to 30-fold relative to the cyclohexane 12, while maintaining selectivity against the RS4;11 cell line. Thus, A-1331852 (13) exhibited a 6 nM EC<sub>50</sub> against the MOLT-4 cell line, a level of *in vitro* efficacy 20-fold more potent than our previously disclosed tool compound A-1155463 (1).

The mechanism-based effects of A-1331852 (13) in MOLT-4 cells were rigorously established, as reported previously.<sup>13</sup> Specifically, treatment of these tumor cells with A-1331852 disrupted BCL-X<sub>L</sub>:BIM complexes and induced classical features of apoptosis including cytochrome *c* release, caspase-3/-7 activation, and externalization of phosphatidylserine as determined by flow cytometric evaluation of Annexin-V staining.<sup>13</sup>

During these studies an X-ray crystal structure of the P4 methoxy-adamantane analog 14 (see Figure 4A) was determined in complex with BCL-X<sub>L</sub>. The complex shown in Figure 4B exhibits the interaction of the 5-methylpyrazole moiety with a lipophilic pocket formed in the binding groove by residues Tyr101, Phe97, and Phe105. The pyrazole:pyridine dihedral angle has increased to 58° and is likely reinforced in the ground state by the 5-methyl pyrazole substitution. More notable, however, is the binding of the adamantane moiety and the consequent displacement of Tyr195 to significantly increase the volume of the P4 pocket (see Tyr195 in Figures 4B–D), which clearly illustrates the elasticity of this binding hot spot.<sup>23</sup>

With the potent and selective BCL-X<sub>L</sub> inhibitor A-1331852 (13) in hand, we evaluated the oral and IV pharmacokinetics in rats and mice, which comprised the primary species for planned investigative toxicology and efficacy experiments, respectively (see Tables 6A and 6B). The pharmacokinetics of A-1331852 upon IV dosing in rats are characterized by 4-h half-life, low total plasma clearance, and low volume of distribution. The oral exposure of A-1331852 in rats following

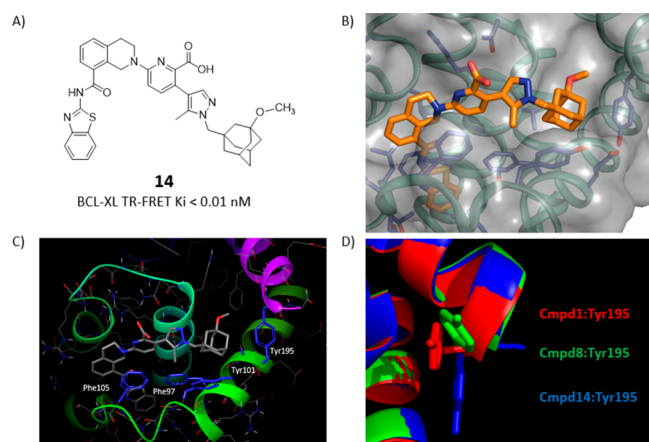


**Figure 4.** (A) Structure and BCL- $X_L$  TR-FRET binding data of compound 14. (B) X-ray structure of compound 14 bound to BCL- $X_L$  protein. The protein is depicted as a ribbon with a gray surface, and key amino acid residues are colored in blue. (C) Alternative depiction of compound 14 bound to BCL- $X_L$  protein. The protein is depicted as a ribbon, and key amino acid residues are labeled and colored blue. (D) Superposition of BCL- $X_L$  Tyr195 when bound to compounds 1 (red ribbon/Tyr195), 8 (green ribbon/Tyr195), and 14 (blue ribbon/Tyr195).

**Table 6.** Select Rat and CD-1 Mouse IV and Oral PK Parameters for A-1331852 (13)

| Table 6A: Rat IV PK, 5 mpk        |                 |                 |                  | Rat PO PK, 5 mpk        |                  |      |
|-----------------------------------|-----------------|-----------------|------------------|-------------------------|------------------|------|
| $t_{1/2}$ (h)                     | $V_{ss}$ (L/kg) | $Cl_p$ (L/h/kg) | AUC ( $\mu$ M-h) | $C_{max}$ ( $\mu$ M)    | AUC ( $\mu$ M-h) | F(%) |
| 3.9                               | 0.18            | 0.08            | 94.9             | 1.97                    | 12.5             | 13   |
| Table 6B: CD-1 Mouse IV PK, 5 mpk |                 |                 |                  | CD-1 Mouse PO PK, 5 mpk |                  |      |
| $t_{1/2}$ (h)                     | $V_{ss}$ (L/kg) | $Cl_p$ (L/h/kg) | AUC ( $\mu$ M-h) | $C_{max}$ ( $\mu$ M)    | AUC ( $\mu$ M-h) | F(%) |
| 2.4                               | 0.43            | 0.22            | 34.5             | 1.46                    | 3.81             | 11   |

a 5 mg/kg dose provided excellent coverage ( $\sim$ 300-fold) of the cellular  $EC_{50}$  despite modest bioavailability. In CD-1 mice, IV clearance of total drug was higher than in rats, with oral  $C_{max}$  exceeding 200-fold the cellular  $EC_{50}$  and similar overall bioavailability as rat. These levels of oral exposure relative to the potency of A-1331852 were deemed sufficient for the use of this molecule in the critical preclinical efficacy and toxicology proof-of-concept studies described previously.<sup>13</sup>

We first embarked on *in vivo* efficacy studies where A-1331852 was dosed as monotherapy or in combination with docetaxel,<sup>13</sup> the results of which have been reported recently. We additionally utilized A-1331852 to evaluate other combinations of BCL- $X_L$  inhibition with standard chemotherapy *in vivo*. We recently reported that *BCL2L1* (BCL- $X_L$ ) amplification characterizes a subset of colorectal cancer (CRC) cell lines, including the Colo205 cell line.<sup>16</sup> Furthermore, *in vitro* knockdown of BCL- $X_L$  protein expression in CRC cells by antisense oligonucleotides can enhance the apoptotic response to topoisomerase I (Topo I) inhibitors,<sup>24</sup> thereby suggesting a potential combination treatment therapy of a small-molecule BCL- $X_L$  inhibitor with a Topo I inhibitor such as irinotecan.

To assess the potential of this combination in an *in vivo* setting, A-1331852 was assessed for efficacy in the Colo205 murine xenograft model of human colorectal cancer as single agent and in combination with irinotecan, as shown in Figure

5. SCID/Beige mice were inoculated with Colo205 cells and size-matched to tumor volumes of approximately 220 mm<sup>3</sup>,

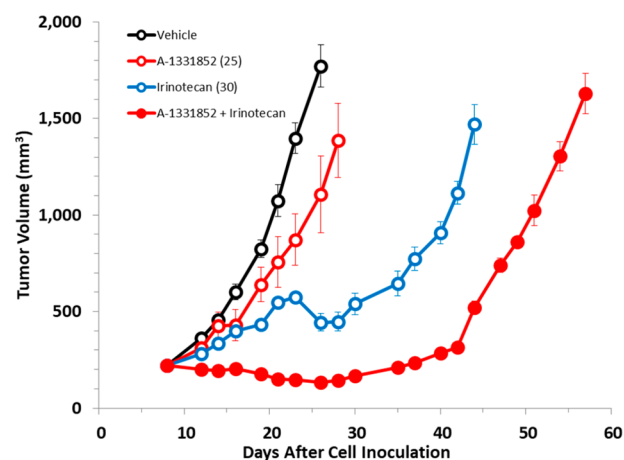


**Figure 5.** Inhibition of Colo205 xenograft tumor growth after treatment with A-1331852 (13) plus irinotecan. Irinotecan was administered IP at 30 mg/kg/day following a Q3D  $\times$  4 regimen. A-1331852 at 25 mg/kg/day was administered PO following a QD  $\times$  14 regimen.

after which A-1331852 was dosed orally as a single agent or in combination with irinotecan.  $TGI_{max}$ -values following treatment with A-1331852 (25 mg/kg/day, QD  $\times$  14) or irinotecan (30 mg/kg/day, Q3D  $\times$  4) were 35 or 75%, respectively. Treatment with a combination of A-1331852 and irinotecan resulted in a  $TGI_{max}$  value of 92%. Thus, tumor growth inhibition following the combination treatment was significantly ( $p < 0.001$ ) higher than after treatment with irinotecan alone. Furthermore, the combination also significantly ( $p < 0.001$ ) increased the durability of the response (TGD = 254%) as compared to that observed after treatment with irinotecan (TGD = 162%) alone.

In summary, we employed structure-based design to generate the first reported selective BCL- $X_L$  inhibitor with oral activity in preclinical models. Specifically, introduction of rigid pyrazole linkers to a THIQ-pyridine core gave rise to an unanticipated mode of binding in the P4 pocket. This binding mode was conducive to the novel introduction of nonaromatic moieties in this region. To this end, incorporation of  $sp^3$ -rich P4 binders led to the generation of A-1331852, a BCL- $X_L$  inhibitor with excellent selectivity and unprecedented cellular potency. These properties, combined with the demonstrated oral exposure in rodents, prompted the nomination of A-1331852 as a key *in vivo* tool compound for testing critical hypotheses underlying the concept of selective BCL- $X_L$  inhibition.<sup>13</sup> Ultimately data from these studies provided preclinical validation for this concept, thus paving the way for a drug discovery program.

## ■ ASSOCIATED CONTENT

### Supporting Information

The Supporting Information is available free of charge at <https://pubs.acs.org/doi/10.1021/acsmchemlett.9b00568>.

Experimental details describing the biological assays, crystallization methods, and the synthesis and characterization of compounds 1–14 (PDF)

PDB coordinates for BCL- $X_L$  in complex with compound 8 (PDF)

PDB coordinates for BCL-X<sub>L</sub> in complex with compound 14 (PDF)

## AUTHOR INFORMATION

### Corresponding Author

**Andrew S. Judd** – AbbVie Inc., North Chicago, Illinois 60064, United States; [orcid.org/0000-0003-2562-8841](https://orcid.org/0000-0003-2562-8841); Email: [andrew.judd@abbvie.com](mailto:andrew.judd@abbvie.com)

### Authors

**Le Wang** – AbbVie Inc., North Chicago, Illinois 60064, United States

**George A. Doherty** – AbbVie Inc., North Chicago, Illinois 60064, United States

**Zhi-Fu Tao** – AbbVie Inc., North Chicago, Illinois 60064, United States

**T. Matthew Hansen** – AbbVie Inc., North Chicago, Illinois 60064, United States

**Robin R. Frey** – AbbVie Inc., North Chicago, Illinois 60064, United States

**Xiaohong Song** – AbbVie Inc., North Chicago, Illinois 60064, United States

**Milan Bruncko** – AbbVie Inc., North Chicago, Illinois 60064, United States

**Aaron R. Kunzer** – AbbVie Inc., North Chicago, Illinois 60064, United States

**Xilu Wang** – AbbVie Inc., North Chicago, Illinois 60064, United States

**Michael D. Wendt** – AbbVie Inc., North Chicago, Illinois 60064, United States

**John A. Flygare** – Genentech, Inc., South San Francisco, California 94080, United States

**Nathaniel D. Catron** – AbbVie Inc., North Chicago, Illinois 60064, United States

**Russell A. Judge** – AbbVie Inc., North Chicago, Illinois 60064, United States

**Chang H. Park** – AbbVie Inc., North Chicago, Illinois 60064, United States

**Shashank Shekhar** – AbbVie Inc., North Chicago, Illinois 60064, United States; [orcid.org/0000-0002-1903-5380](https://orcid.org/0000-0002-1903-5380)

**Darren C. Phillips** – AbbVie Inc., North Chicago, Illinois 60064, United States

**Paul Nimmer** – AbbVie Inc., North Chicago, Illinois 60064, United States

**Morey L. Smith** – AbbVie Inc., North Chicago, Illinois 60064, United States

**Stephen K. Tahir** – AbbVie Inc., North Chicago, Illinois 60064, United States

**Yu Xiao** – AbbVie Inc., North Chicago, Illinois 60064, United States

**John Xue** – AbbVie Inc., North Chicago, Illinois 60064, United States

**Haichao Zhang** – AbbVie Inc., North Chicago, Illinois 60064, United States

**Phuong N. Le** – AbbVie Inc., North Chicago, Illinois 60064, United States

**Michael J. Mitten** – AbbVie Inc., North Chicago, Illinois 60064, United States

**Erwin R. Boghaert** – AbbVie Inc., North Chicago, Illinois 60064, United States

**Wenqing Gao** – AbbVie Inc., North Chicago, Illinois 60064, United States

**Peter Kovar** – AbbVie Inc., North Chicago, Illinois 60064, United States

**Edna F. Choo** – Genentech, Inc., South San Francisco, California 94080, United States; [orcid.org/0000-0003-4200-8302](https://orcid.org/0000-0003-4200-8302)

**Dolores Diaz** – Genentech, Inc., South San Francisco, California 94080, United States

**Wayne J. Fairbrother** – Genentech, Inc., South San Francisco, California 94080, United States

**Steven W. Elmore** – AbbVie Inc., North Chicago, Illinois 60064, United States

**Deepak Sampath** – Genentech, Inc., South San Francisco, California 94080, United States

**Joel D. Levenson** – AbbVie Inc., North Chicago, Illinois 60064, United States

**Andrew James Souers** – AbbVie Inc., North Chicago, Illinois 60064, United States

Complete contact information is available at:

<https://pubs.acs.org/10.1021/acsmmedchemlett.9b00568>

### Author Contributions

The manuscript was written through contributions of all authors. All authors have given approval to the final version of the manuscript.

### Funding

The design, study contact, and financial support for this research were provided by AbbVie and Genentech, a member of the Roche group.

### Notes

The authors declare the following competing financial interest(s): AbbVie and Genentech participated in interpretation of data and review and approval of publication. L.W., G.A.D., A.S.J., Z-F.T., T. M. H., R.R.F., X.S., M.B., A.R.K., X.W., M.D.W., N.D.C., S.S., D.C.P., R.A.J., P.N., M.L.S., S.K.T., Y.X., J.X., H.Z., P.N.L., M.J.M., E.R.B., W.G., P.K., S.W.E., J.D.L., and A.J.S. are employees of AbbVie, Inc. C.H.P. was an employee of AbbVie, Inc at the time of the study. E.C. and W.J.F. are employees of Genentech, Inc. J.A.F., D.D., and D.S. were employees of Genentech, Inc. at the time of the study.

### Biography

Andrew S. Judd received his Ph.D. degree from the University of Minnesota-Twin Cities under the guidance of Prof. Thomas R. Hoye. Subsequently he joined the research group of Prof. Stephen F. Martin at the University of Texas at Austin as an NIH Postdoctoral Fellow. Andrew began his industry career as part of Abbott Laboratories Metabolic Disease Research Division in 2002. Subsequently he has worked in Oncology Research since 2007 for Abbott Laboratories and AbbVie, Inc. His research interests include apoptosis, protein-protein interactions, and antibody-drug conjugates.

## ACKNOWLEDGMENTS

We gratefully acknowledge the contributions of Gerard M. Sullivan to the synthesis and design of selective BCL-X<sub>L</sub> inhibitors. X-ray diffraction data were collected at beamline 17-ID in the facilities of the Industrial Macromolecular Crystallography Association Collaborative Access Team (IMCA-CAT) at the Advanced Photon Source. These facilities are supported by the companies of the Industrial Macromolecular Crystallography Association. The Advanced Photon Source, an Office of Science User Facility, is operated



for the U.S. Department of Energy (DOE) Office of Science by Argonne National Laboratory.

## DEDICATION

This manuscript is dedicated to the memory of our dear colleague, Gerard M. Sullivan (12/7/1957–12/18/2017).

## ABBREVIATIONS

AUC, area under the curve; FRET, fluorescence resonance energy transfer; IV, intravenous; mpk, milligram per kilogram; PO, *per os*, from the Latin for “by mouth”; PK, pharmacokinetics; QD, *quaque die*, from the Latin for “once in a day”; TGD, tumor growth delay; TGI, tumor growth inhibition

## REFERENCES

- (1) Oltersdorf, T.; Elmore, S. W.; Shoemaker, A. R.; Armstrong, R. C.; Augeri, D. J.; Belli, B. A.; Bruncko, M.; Deckworth, D. L.; Dinges, J.; Hajduk, P. J.; Joseph, M. K.; Kitada, S.; Korsmeyer, S. J.; Kunzer, A. R.; Letai, A.; Li, C.; Mitten, M. J.; Nettesheim, D. G.; Ng, S.; Nimmer, P. M.; O'Connor, J. M.; Oleksijew, A.; Petros, A. M.; Reed, J. C.; Shen, W.; Tahir, S. K.; Thompson, C. B.; Tomaselli, K. J.; Wang, B.; Wendt, M. D.; Zhang, H.; Fesik, S. W.; Rosenberg, S. H. An Inhibitor of BCL-2 Family Proteins Induces Regression of Solid Tumours. *Nature* **2005**, *435*, 677–681.
- (2) Tse, C.; Shoemaker, A. R.; Adickes, J.; Anderson, M. G.; Chen, J.; Jin, S.; Johnson, E. F.; Marsh, K. C.; Mitten, M. J.; Nimmer, P.; Roberts, L.; Tahir, S. K.; Xiao, Y.; Yang, X.; Zhang, H.; Fesik, S.; Rosenberg, S. H.; Elmore, S. W. ABT-263: A Potent and Orally Bioavailable BCL-2 Family Inhibitor. *Cancer Res.* **2008**, *68*, 3421–3428.
- (3) Shoemaker, A. R.; Mitten, M. J.; Adickes, J.; Ackler, S.; Refici, M.; Ferguson, D.; Oleksijew, A.; O'Connor, M.; Wang, B.; Frost, D. J.; Bauch, J.; Marsh, K.; Tahir, S. K.; Yang, X.; Tse, C.; Fesik, S. W.; Rosenberg, S. H.; Elmore, S. W. Activity of the BCL-2 Family Inhibitor ABT-263 in a Panel of Small Cell Lung Cancer Xenograft Models. *Clin. Cancer Res.* **2008**, *14*, 3268–3277.
- (4) Ackler, S. L.; Mitten, M. J.; Foster, K.; Oleksijew, A.; Refici, M.; Tahir, S. K.; Xiao, Y.; Tse, C.; Frost, D. J.; Fesik, S. W.; Rosenberg, S. H.; Elmore, S. W.; Shoemaker, A. R. The BCL-2 Inhibitor ABT-263 Enhances the Response of Multiple Chemotherapeutic Regimens in hematologic Tumors *In vivo*. *Cancer Chemother. Pharmacol.* **2010**, *66*, 869–880.
- (5) Chen, J.; Jin, S.; Abraham, V.; Huang, X.; Liu, B.; Mitten, M.; Nimmer, P.; Lin, X.; Smith, M.; Shen, Y.; Shoemaker, A. R.; Tahir, S. K.; Zhang, H.; Ackler, S. L.; Rosenberg, S. H.; Maecker, H.; Sampath, D.; Levenson, J. D.; Tse, C.; Elmore, S. W. The BCL-2/BCL-X<sub>L</sub>/BCL-w Inhibitor, Navitoclax, Enhances the Activity of Chemotherapeutic Agents *in vitro* and *in vivo*. *Mol. Cancer Ther.* **2011**, *10*, 2340–2349.
- (6) Wilson, W. H.; O'Connor, O. A.; Czuczman, M. S.; LaCasce, A. S.; Gerecitano, J. F.; Leonard, J. P.; Tulpule, A.; Dunleavy, K.; Xiong, H.; Ciu, Y.-L.; Cui, Y.; Busman, T.; Elmore, S. W.; Rosenberg, S. H.; Krivoshik, A. P.; Enschede, S. H.; Humerickhouse, R. A. Navitoclax, A Targeted High-Affinity Inhibitor of BCL-2, in Lymphoid Malignancies: A Phase 1 Dose-Escalation Study of Safety, Pharmacokinetics, Pharmacodynamics, and Anti-tumor Activity. *Lancet Oncol.* **2010**, *11*, 1149–1159.
- (7) Roberts, A. W.; Seymour, J. F.; Brown, J. R.; Wierda, W. G.; Kipps, T. J.; Khaw, S. L.; Carney, D. A.; He, S. Z.; Huang, D. C. S.; Xiong, H.; Cui, Y.; Busman, A.; McKeegan, E. M.; Krivoshik, A. P.; Enschede, S. H.; Humerickhouse, R. Substantial Susceptibility of Chronic Lymphocytic Leukemia to BCL-2 Inhibition: Results of Phase I Study of Navitoclax in Patients with Relapsed or refractory Disease. *J. Clin. Oncol.* **2012**, *30*, 488–496.
- (8) Zhang, H.; Nimmer, P.; Tahir, S. K.; Chen, J.; Fryer, R. M.; Hahn, K. R.; Iciek, L. A.; Morgan, S. J.; Nasarre, M. C.; Nelson, R.; Preusser, L. C.; Reinhart, G. A.; Smith, M. L.; Rosenberg, S. H.; Elmore, S. W.; Tse, C. BCL-2 Family Proteins Are Essential for Platelet Survival. *Cell Death Differ.* **2007**, *14*, 943–951.
- (9) Mason, K. D.; Carpinelli, M. R.; Fletcher, J. I.; Collinge, J. E.; Hilton, A. A.; Ellis, P.; Kelly, P. N.; Ekert, P. G.; Metcalf, D.; Roberts, A. W.; Huang, D. C. S.; Kyle, B. T. Programmed Anuclear Cell Death Delimits Platelet Life Span. *Cell* **2007**, *128*, 1173–1186.
- (10) Souers, A. J.; Levenson, J. D.; Boghaert, E. R.; Ackler, S. L.; Catron, N. D.; Chen, J.; Dayton, B. D.; Ding, H.; Enschede, S. H.; Fairbrother, W. J.; Huang, D. C. S.; Hymowitz, S. G.; Jin, S.; Khaw, S. L.; Kovar, P. J.; Lam, L. T.; Lee, J.; Maecker, H. L.; Marsh, K. C.; Mason, K. D.; Mitten, M. J.; Nimmer, P. M.; Oleksijew, A.; Park, C. H.; Park, C. M.; Phillips, D. C.; Roberts, A. W.; Sampath, D.; Seymour, J. F.; Smith, M. L.; Sullivan, G. M.; Tahir, S. K.; Tse, C.; Wendt, M. D.; Xiao, Y.; Xue, J. C.; Zhang, A. R.; Humerickhouse, R. A.; Rosenberg, S. H.; Elmore, S. W. ABT-199, A Potent and Selective BCL-2 Inhibitor, Achieves Anti-tumor Activity While Sparing Platelets. *Nat. Med.* **2013**, *19*, 202–208.
- (11) Seymour, J. F.; Davids, M. S.; Pagel, J. M.; Kahl, B. S.; Wierda, W. G.; Puvvada, S.; Gerecitano, J. F.; Kipps, T. J.; Anderson, M. A.; Huang, D. C. S.; Rudersdorf, N.; Gressick, L. A.; Montalvo, N. P.; Yang, J.; Zhu, M.; Dunbar, M.; Cerri, E.; Enschede, S. H.; Humerickhouse, R.; Roberts, A. W. ABT-199 (GDC-0199) in Relapsed/Refractory (R/R) Chronic Lymphocytic Leukemia (CLL) and Small Lymphocytic Lymphoma (SLL): High Complete Response Rate and Durable Disease Control. *J. Clin. Oncol.* **2014**, *32*, 7015.
- (12) Puglisi, M.; van Doorn, L.; Blanco-Codesido, M.; De Jonge, M. J.; Moran, K.; Yang, J.; Busman, T.; Franklin, C.; Mabry, M.; Krivoshik, A.; Humerickhouse, R.; Molife, L. R.; Eskens, F. A Phase I Safety and Pharmacokinetic (PK) Study of Navitoclax (N) in Combination with Docetaxel (D) in Patients (pts) with solid Tumors. *J. Clin. Oncol.* **2011**, *29*, 2518.
- (13) Levenson, J. D.; Phillips, D. C.; Mitten, M. J.; Boghaert, E. R.; Diaz, D.; Tahir, S. K.; Belmont, L. D.; Nimmer, P.; Xiao, Y.; Ma, X. M.; Lowes, K. M.; Kovar, P.; Chen, J.; Jin, S.; Smith, M.; Xue, J.; Zhang, H.; Oleksijew, A.; Magoc, T. J.; Vaidya, K. S.; Albert, D. H.; Tarrant, J. M.; La, N.; Wang, L.; Tao, Z.-F.; Wendt, M. W.; Sampath, D.; Rosenberg, S. H.; Tse, C.; Huang, D. C. S.; Fairbrother, W. J.; Elmore, S. W.; Souers, A. J. Exploiting Selective BCL-2 Family Inhibitors to dissect Cell Survival Dependencies and Define Improved Strategies for Cancer Therapy. *Sci. Transl. Med.* **2015**, *7*, 279ra4027ra40.
- (14) Tao, Z.-F.; Hasvold, L.; Wang, L.; Wang, X.; Petros, A. M.; Park, C. H.; Boghaert, E. R.; Catron, N. D.; Chen, J.; Colman, P. M.; Czabotar, P. E.; Deshayes, K.; Fairbrother, W. J.; Flygare, J. A.; Hymowitz, S. G.; Jin, S.; Judge, R. A.; Koehler, M. F. T.; Kovar, P. J.; Lessene, G.; Mitten, M. J.; Ndubaku, C. O.; Nimmer, P.; Purkey, H. E.; Oleksijew, A.; Phillips, D. C.; Sleebs, B. E.; Smith, B. J.; Smith, M. L.; Tahir, S. K.; Watson, K. G.; Xiao, Y.; Xue, J.; Zhang, H.; Zobel, K.; Rosenberg, S. H.; Tse, C.; Levenson, J. D.; Elmore, S. W.; Souers, A. J. Discovery of Potent and Selective BCL-X<sub>L</sub> Inhibitor with *In vivo* Activity. *ACS Med. Chem. Lett.* **2014**, *5*, 1088–1093.
- (15) Levenson, J. D. Chemical Parsing: Dissecting Cell Dependencies with a Toolkit of Selective BCL-2 Inhibitors. *Molecular & Cellular Oncology* **2016**, *3*, e1050155/1–e1050155/2.
- (16) Zhang, H.; Xue, J.; Hessler, P.; Tahir, S. K.; Chen, J.; Jin, S.; Souers, A. J.; Levenson, J. D.; Lam, L. T. Genomic Analysis and Selective Small Molecule Inhibition Identifies BCL-X<sub>L</sub> as a Critical Survival Factor in a Subset of Colorectal Cancer. *Mol. Cancer* **2015**, *14*, 1–9.
- (17) Koehler, M. F. T.; Bergeron, P.; Choo, E. F.; Lau, K.; Ndubaku, C.; Dudley, D.; Gibbons, P.; Sleebs, B. E.; Rye, C. S.; Nikolakopoulos, G.; Bui, C.; Kulasegaram, S.; Kersten, W. J. A.; Smith, B. J.; Czabotar, P. E.; Colman, P. M.; Huang, D. C. S.; Baell, J. B.; Watson, K. G.; Hasvold, L.; Tao, Z.-F.; Wang, L.; Souers, A. J.; Elmore, S. W.; Flygare, J. A.; Fairbrother, W. J.; Lessene, G. Structure-guided Rescaffolding of Selective Antagonists of BCL-X<sub>L</sub>. *ACS Med. Chem. Lett.* **2014**, *5*, 662–667.

(18) Lessene, G.; Czabotar, P. E.; Sleebs, B. E.; Zobel, K.; Lowes, K. M.; Adams, J. A.; Baell, J. B.; Colman, P. M.; Deshayes, K.; Fairbrother, W. J.; Flygare, J. A.; Gibbons, P.; Kersten, W. J. A.; Kulasegaram, S.; Moss, R. M.; Parisot, J. P.; Smith, B. J.; Street, I. P.; Yang, H.; Huang, D. S. C.; Watson, K. G. Structure-guided Design of a Selective BCL-X<sub>L</sub> Inhibitor. *Nat. Chem. Biol.* **2013**, *9*, 390–397.

(19) Veber, D. F.; Johnson, S. R.; Cheng, H. Y.; Smith, B. R.; Ward, K. W.; Kopple, K. D. Molecular Properties that Influence the Oral Bioavailability of Drug Candidates. *J. Med. Chem.* **2002**, *45*, 2615–2623.

(20) Lee, E. F.; Czabotar, P. E.; Smith, B. J.; Deshayes, K.; Zobel, K.; Colman, P. M.; Farlie, W. D. Crystal Structure of ABT-737 Complexed with BCL-XL: Implications for Selectivity of Antagonists of the BCL-2 Family. *Cell Death Differ.* **2007**, *14*, 1711–1713.

(21) Lovering, F.; Bikker, J.; Humblet, C. Escape from Flatland: Increasing Saturation as an Approach to Improving Clinical Success. *J. Med. Chem.* **2009**, *52*, 6752–6756.

(22) Lovering, F. Escape from Flatland 2: Complexity and Promiscuity. *MedChemComm* **2013**, *4*, 515–519.

(23) Wang, S.; Yang, C.-Y. Hydrophobic Binding Hot Spots of BCL-XL Protein-Protein Interfaces by Cosolvent Molecular dynamics Simulation. *ACS Med. Chem. Lett.* **2011**, *2*, 280–284.

(24) Hayward, R. L.; Macpherson, J. S.; Cummings, J.; Monia, B. P.; Smyth, J. F.; Jodrell, D. I. Antisense BCL-XL Down-regulation Switches the Response of Topoisomerase I Inhibition from Senescence to Apoptosis in Colorectal Cancer Cells, Enhancing Global Cytotoxicity. *Clin. Cancer Res.* **2003**, *9*, 2856–2865.